Nov 16th, 12:00 AM

The Post Buckling Behaviour of Bending Elements

J. Rhodes

THE POST BUCKLING BEHAVIOUR OF BENDING ELEMENTS

by

J Rhodes (1)

INTRODUCTION

The effects of local buckling on the behaviour of bending elements of thin walled sections has received a great deal of research attention in recent years. As the buckling stresses for such elements are in general substantially higher than for compression elements buckling analysis was, before the last decade or so, limited to evaluation of the critical stress. However, in order to use webs with high depth to thickness ratios it has been recognised that the reduction in effectiveness caused by buckling must be taken into account if safe design is to be ensured.

In the case of stiffened elements a great deal of research has been carried out in Sweden (1), (2), (3) and in the United States (4), (5), into the effects of in-plane bending, and a number of different design analysis procedures have been formulated. Most of these employ the concept of 'effective width' as for compression element analysis, with a variety of suggested effective width values and positions being proposed for design computation.

The use of the effective width approach for bending elements is a more difficult task than for compression elements, as the positions of the effective portions of the element width affects the bending behaviour. It is also more difficult to justify theoretically the use of the effective width approach for bending elements since there are mathematical reasons which preclude complete compliance of any effective width set-up with the results of rigorous analysis.

In the case of unstiffened elements which are subject to bending which causes compression of the free edge the effects of local buckling can be quite dramatic in altering the in-plane flexural behaviour. The AISI specification (6) permits only extremely limited use of such elements as parts of columns etc., in the post-buckling range.

(1) Senior Lecturer, University of Strathclyde, Glasgow, Scotland.

In this paper the behaviour of bending elements is investigated analytically for the cases of stiffened and unstiffened elements. In both cases the conditions of simple support and full fixity of the supported unloaded edges are considered.

OUTLINE OF THEORETICAL ANALYSIS

A portion of plate between two buckle nodes is shown in Fig. 1. Due to the applied moment the displacement system varies linearly from $u^*(1 - \alpha)$ at the tension edge (edge 1) to u^* at the compression edge (edge 2). Here α defines the position of the neutral axis which is a distance b/α from the compression edge. The effects of other elements of a section on the one under consideration is in general to subject this element to an additional axial force, as indicated in the figure, which will also change the position of the neutral axis.

In the case of an isolated plate, α has the value 2 before local buckling and the neutral axis is at the plate centre line. After buckling the neutral axis position changes.

The method of analysis used was the semi-energy method. This method has been described in previous papers (7), (8) and will only be very briefly outlined here as follows:-

Firstly, for a plate under a given end displacement system such as that of Fig. 1 a form for the local buckles is postulated with unknown coefficents specifying the deflection magnitudes. This is then used in conjunction with von Karman's compatibility equation to obtain the corresponding stress system in terms of the deflection coefficient and the end displacements. The total potential energy can then be written in terms of the deflection coefficients and application of the Principle of Minimum Potential energy furnishes the required relationships between the deflection magnitudes and the end displacements. Knowing these relationships the stresses can be evaluated for the given end displacements and the corresponding applied load and moment thus obtained.

The accuracy of the method relies solely on the capability of the assumed deflection system to adequately describe the true deflected form, and, of course, the limitations of plate large deflection theory. To ensure that the assumed deflected form is accurate in its description of the buckle shape a rigorous analysis of the local buckling situation is first carried out and the buckled form obtained from this is then postulated as that which holds in the immediate post-buckling range. If it is assumed that this shape remains constant and only the magnitude of the local buckles change then simple expressions covering the plate behaviour can be obtained. This assumption was made as a first step, and the accuracy of the solution was checked in the post-buckling range by allowing changes in the deflected form.

On the assumption of a non-changing deflection shape the relationships derived between out of plane deflections, w, the end displacement parameters u* and α and the applied load P and the moment M calculated about the tension edge are of the following form

$$(^{w}/_{t})_{max} = A\left(\frac{M}{M_{CR}} - 1\right)^{\frac{1}{2}} \tag{1}$$

$$\frac{P}{P_{CR}} = C_1 \frac{u^*}{u_{CR}} - C_2 \frac{u^*\alpha}{u_{CR}} + (1 - C_1) \tag{2}$$

$$\frac{M}{bP_{CR}} = C_3 \frac{u^*}{u_{CR}} - C_4 \frac{u^*\alpha}{u_{CR}} + (\tfrac{1}{2} - C_3) \tag{3}$$

The constants C_1 - C_4 are obtained from the energy expressions and depend on the deflected shape. P_{CR} and u_{CR} are the buckling load and displacement under pure compression which is obtained using this deflected shape.

The corresponding expressions for a non-buckled plate, w = 0, are

$$\frac{P}{P_{CR}} = \frac{u^*}{u_{CR}} - \frac{1}{2}\frac{u^*\alpha}{u_{CR}} \tag{4}$$

$$\frac{M}{bP_{CR}} = \tfrac{1}{2}\frac{u^*}{u_{CR}} - \frac{1}{6}\frac{u^*\alpha}{u_{CR}} \tag{5}$$

Equations (4) and (5) are particular cases of (2) and (3) with $C_1 = 1,\ C_2 = C_3 = \frac{1}{2}\ \ C_4 = \frac{1}{6}$

Examining equations (2) and (3) and comparing with (4) and (5) shows that the various plate properties, compressional stiffness, bending rigidity, neutral axis position etc which can be obtained for the unbuckled plate can also be obtained for the buckled plate, with altered values. For example with α set equal to zero, i.e. pure compression, equation (4) gives

$$\partial P/\partial u^* = P_{CR}/u_{CR}$$

indicating linearity of the load end displacement curve before buckling. Equation (2) on the other hand gives, with $\alpha = 0$,

$$\partial P/\partial u^* = C_1\ P_{CR}/u_{CR}$$

This indicates linearity of the post-buckling load end displacement curve, but with a different slope.

Manipulation of these equations enables the other plate properties, I and $\bar{y}$ to be obtained in a similar fashion for the pre-buckling and post-buckling situations. The values obtained in this way are termed 'tangent' values, having been obtained by examining the slopes of the displacements etc, e.g. $\partial P/\partial u^*$ and the ratio of post-buckling to pre-buckling values are in all cases constant, because of the non-changing buckled form assumption. To illustrate this, the ratio of $\partial P/\partial u^*$ after buckling to that before buckling is C_1, and this quantity defines the tangent compressional stiffness after buckling as a ratio of that before buckling. This is often expressed in terms of an effective Young's modulus E^*, such that

$$\frac{E^*}{E} = C_1 \qquad (6)$$

Similar relationships between tangent flexural stiffness, I^* and I, tangent neutral axis position $\bar{y}^*$ and $\bar{y}$, can be obtained from eqns. (2) - (5).

These tangent values are only applicable to that part of the load or moment applied after buckling, and the total load applied must be computed as the sum of pre-buckling and post-buckling components. To overcome this 'secant' values are often used, in which case the element has an effective resistance to the various actions which varies with loading. For example returning to the case of $\alpha = 0$, equation (2) gives

$$P = C_1 \quad u^* \quad \frac{P_{CR}}{u_{CR}} + (1 - C_1) \quad P_{CR}.$$

The secant stiffness, say E_{eff} can be written as the ratio of P calculated on the basis of a buckled element to that determined on the basis of an unbuckled element

$$\frac{E_{eff}}{E} = C_1 + (1 - C_1)\frac{u_{CR}}{u^*} = \frac{E^*}{E} + (1 - \frac{E^*}{E})\frac{u_{CR}}{u^*} \qquad (7)$$

E_{eff}/E is generally referred to when dealing with the compression case as be/b, the ratio of effective to full width of the plate. This is perfectly justifiable for the case of pure compression, but in situations where bending is also present it introduces constraints which are not present in the theoretical derivation because of the subsequent necessity to detail the position of the effective width. Therefore, on order to deal with an effective element property, rather than an effective material property, such as E_{eff} the ratio E_{eff}/E will in this paper be referred to as A_{eff}/A, i.e. an effective area. This eliminates the problems arising with the specification of an effective width.

In a similar manner the ratios of I_{eff}/I and $\bar{y}_{eff}/\bar{y}$ can be written in terms of their tangent values and the ratio u^*/u_{CR}.

The values so obtained are accurate in the immediate post-buckling range, but as buckling progresses account must be taken of further gradual changes in the properties.

THEORETICAL RESULTS

Theoretical results are presented and discussed here for four particular cases. These are:-

Case 1 Edges 1 and 2 simply supported
Case 2 Edges 1 and 2 fixed
Case 3 Edge 1 simply supported, edge 2 free
Case 4 Edge 1 fixed edge 2 free

a). Buckling Stresses

The value of the compression edge stress at buckling may be expressed in the form

$$\sigma_{CR} = K\frac{\pi^2 E\ (t/b)^2}{12\ (1 - \nu^2)} \tag{8}$$

Ref (4) quotes an expression for the K factors for case 1 which may be written as

$$K = 4 + 2\alpha + 2\alpha^3 \tag{9}$$

This expression gives accurate values for $\alpha < 2$, but for higher values of α the buckling coefficients err on the high side. For $\alpha = 3$ eqn 9 gives $K = 64$, whereas it can be shown that an upper bound value for K when $\alpha > 2$ is given by

$$K = 6\ \alpha^2 \tag{10}$$

For practical purposes it is suggested that eqn (9) be used for $\alpha < 2$ and eqn (10) for $\alpha > 2$. When $\alpha = 3$ the factor K obtained from (10) is 54.

An alternative expression which agrees well with the results of the theoretical investigation for both cases (1) and (2) is

$$K = K_o\ (1 + 0.9\ \alpha^{2.4}) \tag{11}$$

where $K_o = 4$ for case 1 and 6.97 for case 2.

For case 3 the buckling coefficient may be approximated to by

$$K = 0.425/(1 - \alpha/4) \tag{12}$$

and for case 4 the corresponding expression is

$$K = 1.28/(1 - \alpha/5) \tag{13}$$

These expressions give buckling coefficients in all cases within 3% of theoretically calculated values if $\alpha < 3$. It is rather difficult to imagine a situation in which an unstiffened element of a section could be loaded with $\alpha > 2$ except if the section was under a combination of tension and bending.

The variation of buckling coefficient with buckle half wavelength is shown in Fig.2 for the particular case of pure bending, $\alpha = 2$. The post-buckling results given subsequently are based on plates which sustain the minimum buckling stresses given in Fig.2. Thus the approximate buckle half wavelengths considered were a/b = 0.69 for case 1, a/b = 0.5 for case 2, a/b = 1.65 for case 4. For case 3 the value of K decreases indefinitely with a/b so a value of a/b = 2 was arbitrarily selected for examination.

b) Initial Post-buckling behaviour

Fig.3 shows the deflected form across the plate for all four cases and Fig.4 shows the variation of membrane stresses across the plate for each case at an applied moment approaching twice that to cause local buckling. For cases 1 and 2 the variation of stresses along the length of the element is negligible on the tension side and only becomes significant near the compression edge.

For cases 3 and 4 the stress variations are markedly different from those obtained before buckling. The free edges shed load at a high rate and there is a tendency for these edges to sustain tensile stresses at high moments.

Fig.5 shows the variation in maximum deflection with variation in moment for the different cases. The results are shown in terms of M/M_{CR}, but it should be noted that the critical moments for each case are widely different. As can be seen the maximum deflections of plates with free edges increase at a much faster rate than the others.

In Fig.6 the variation of curvature with applied moment is shown. For cases 1 and 2 the reduction in flexural stiffness is much less than is the reduction in compressional stiffness of the same plates under uniform compression. For cases 3 and 4 however the flexural stiffnesses decrease very substantially after buckling and it would not be expected that these plates would have any great deal of post-buckling capacity under normal circumstances.

These results, based on a non-changing deflected form, are summarised in Table 1.

c) Effects of changing deflected form

If the deflected form is allowed to change in the post-buckling range the values of I^*, A^*, $\bar{y}^*$ etc vary in such a way that in general the post-buckling efficiency becomes less than that predicted just after buckling. There are two major factors which cause these effects, change in deflected form across the plate and change in the half wavelength of the buckles. In a long plate it is quite possible for the buckle pattern to self adjust so that the buckle lengths at the most highly stressed section are such as to produce the most adverse effects. For safe analysis therefore the effects of changes in wavelength should be taken into account.

Fig.7 shows the moment curvature variations for cases 1 and 4 to illustrate these effects. As can be seen these can be substantial when the moment becomes much greater than M_{CR}.

d) Effects of imperfections

It is well known that local imperfections can have significant effects and should be taken into account. These in general have the effect of masking the buckling load or moment and causing merging of the pre and post-buckling curves. By specifying values of imperfection magnitude the effects can be analysed rigorously using the methods of Ref (8). However, for commercial type elements in which the imperfection magnitudes vary from section to section some generalised method of accounting for imperfections is preferable.

A simple method of accomplishing this is to modify the variation of the effective properties so that these gradually change from the start of loading. The variation of these effective properties, for the perfect plate is as in eqn (7) i.e.

$$\frac{A_{eff}}{A} = \frac{E^*}{E} + \left(1 - \frac{E^*}{E}\right) \frac{u_{CR}}{u^*} \qquad (14)$$

When $u^* = u_{CR}$ $A_{eff}/A = 1$ and this equation must be replaced by $A_{eff}/A = 1$ for $u^* < u_{CR}$. If the term u_{CR}/u^* is replaced by $(1 + u^*/u_{CR})^{-\frac{1}{2}}$ then the equation becomes

$$\frac{A_{eff}}{A} = \frac{E^*}{E} + \left(1 - \frac{E^*}{E}\right)/\left(1 + \frac{u^*}{u_{CR}}\right)^{\frac{1}{2}} \qquad (15)$$

This is applicable for all values of u^*/u_{CR} and gives $A/A_{eff} = 1$ when $u^* = 0$ and approaches the perfect plate values as u^* increases in very much the same way as theoretical analysis predicts.

It is worthy of note here that there is a significant need for some method of analysis particularly for stiffened panels. In most bending members with stiffened web elements the compression flange will buckle locally before the web and thus induce premature web deflections. These have similar effects on the web behaviour as would be caused by imperfections, and the generalised imperfection analysis must be capable of taking these into account.

PRACTICAL APPLICATIONS - UNSTIFFENED PLATES

The use of beams which have unstiffened bending elements with their free edge in compression is not a particulary practical proposition if the unstiffened elements are thin, since the post-buckling flexural rigidity is so low. It is worthy of note that for this type of element the deflected form due to compression is not significantly different from that due to the type of moment action under consideration, so that the tangent properties given in Table 1 for unstiffened elements are applicable to all combination of bending and compression.

In the case of a section loaded in pure bending with unstiffened element in bending the tangent values of the effective properties of this element may be taken directly from Table 1, i.e. $A^*/A = 0.451$. $I^*/I = 0.09$ and $\bar{y}^*/b = 0.196$ measured from the tension edge. Using these properties in the analysis of say a T beam or plain channel shows that the reduction in tangent flexural stiffness of the section after local buckling is of a similar magnitude to that of the bending element itself. Thus after local buckling such a beam retains less than 10% of its initial flexural rigidity. This, combined with the large local deflections induced by buckling makes any post-buckling reserve of load carrying capacity in such circumstances very small.

Probably of greater importance in this case is the effect of local buckling on columns with unstiffened bending elements. Since Euler buckling is dependent on the tangent flexural stiffness then if this reduces to less than 1/10th of its initial value at buckling the Euler load is reduced by the same amount. This situation has been examined in Ref (9) for the case of plain channels and it has shown that even very short columns can fail elastically by Euler buckling due to the huge reductions in flexural stiffness caused by local buckling.

PRACTICAL APPLICATIONS - STIFFENED ELEMENTS

For purposes of assessing the accuracy of results obtained on the basis of pure moments applied to the webs it was decided to examine the results of tests on members which have bending elements which initially undergo pure moment, i.e. box type members. A number of tests on such members carried out by Kallsner, are described in Ref (2). Also de Wolfe et al (5) gave results of tests on 8 beams 4 of which had web members undergoing more or less pure bending initially. These tests were selected as suitable for checking the validity of the analysis.

For comparison purposes the values of tangent moduli and neutral axis positions selected for the analytical web element model were those obtained from case (1), simply supported edges, at a value of moment approximately two and one half times the buckling moment, or three and one half times the critical curvature.

The rounded off values so obtained were

$$\frac{E^*}{E} = 0.5, \quad \frac{I^*}{I} = 0.5, \quad \bar{y}^* = 0.32\ b$$

Using these values together with the imperfection procedure previously mentioned gives, for the effective web parameters to used in calculation

$$A_{eff} = (0.5 + 0.5/(1 + (\frac{\sigma^*}{\sigma_{CR}})^2)^{\frac{1}{2}})\ A \qquad (16)$$

$$I_{eff} = (0.5 + 0.5/(1 + (\frac{\sigma^*}{\sigma_{CR}})^2)^{\frac{1}{2}})\ I \qquad (17)$$

$$\bar{y}_{eff} = (0.32 + 0.18/(1 + (\frac{\sigma^*}{\sigma_{CR}})^2)^{\frac{1}{2}})\ b \qquad (18)$$

Here σ^*, the average compression edge stress is used instead of u^* as the ratio of σ^*/σ_{CR} is the same as u^*/u_{CR}. Note that this neglects the periodic variation of stress along the beam. It has been found previously (10), (11) that this effect is reduced in the consideration of beams from that obtained in the consideration of single plates, so that the maximum and average stresses are not substantially different. The fact that slightly conservative values have been chosen for the effective web parameters makes the assumption that maximum and average edge stresses are equal reasonably safe.

Now equations (16), (17) and (18) can be used in evaluation of the section properties. These can be evaluated, in the normal way, using the parallel axes theorem for each individual element. For the bending elements the actual areas, I values and neutral axis positions are replaced by the effective values given above.

In computing section properties for comparison with the experimental results the tension elements were assumed fully effective, the bending elements were considered to have properties as given by equations (16) - (18) above and the compression elements were considered to have an effective width as given by the AISI specification. The maximum moment was assumed to occur when σ^* became equal to σ_Y, the yield stress and the ratios of experimental to theoretical maximum moments so obtained are plotted against the ratio of σ_Y to σ_{CR} in Fig.8. The buckling coefficient was taken as 24 in evaluation of σ_{CR}. The agreement obtained between analysis and experiment is very good with the analytical values of M_{max} being slightly conservative in the main, but all predictions being within 10% of the experimental failure moments.

Also shown is a curve which represents the increase in maximum moment which would be theoretically obtained if buckling effects on the bending elements were neglected, but the compression flange buckling effects were still taken into account. Thus the difference between this curve and the line M_{max} (exp)/M_{max} (TH) = 1 shows the effect on calculated maximum moment of neglecting web buckling effects. To obtain a single curve such as that given a single geometrical shape must be used. The shape used in this instance was a box-section with web width equal to twice the flange widths and the thickness adjusted to give the required

σ_Y to σ_{CR} ratio, this being rather typical of the sections investigated here.

WEBS WITH COMBINED BENDING AND AXIAL LOAD

An analytical study or elements subject to combined bending and axial compression of tension shows that in general, so long as the axial force is low enough to ensure that the stresses change sign between top and bottom edge, equations (14) - (16) can be used with reasonable accuracy and conservatism for stiffened elements. The buckling stress of course, varies substantially with position of the neutral axis as discussed previously.

Fig.9 shows comparison of the predictions obtained using equations (16) - (18) together with (9) for α less than 2 and (10) for α greater than 2, with the experimental results shown in Fig.9 and also the results of Thomassen, from ref (2) and from ref (5) for the cases where the areas of tension and compression elements were not equal.

This figure shows that the method used gives conservative results for the more general case. Since many of the additional results are for sections which have extremely small web buckling effects the conservatism is due to factors other than any inaccuracy in the analysis of these effects. As the majority of the additional results were for low values of σ_Y/σ_{CR} these results are not so useful in verifying the general accuracy as those of Fig.8. The one result which is substantially less than predicted theoretically is that obtained for the highest value of σ_Y/σ_{CR} by de Wolfe (5). This experimental result may be artificially low due to some unknown experimental factor, or it may signify that the effective properties used in analysis were not accurate in dealing with such a high post-buckling effect. While it may be the case that this experimental result was perhaps lower than expected, it is also probably true that the effective properties used are not suitable for this post-buckling range. In view of this it is suggested that the properties given are suitable for the range $0 < \sigma_Y/\sigma_{CR} < 8$. Relating this to material width to thickness ratios, in the case of webs with yield stress of 250 MN/m^2 (36.3 $kips/in^2$) under pure bending ($K = 24$) then the maximum b/t ratio which can be analysed with accuracy using these properties is 370.

SUMMARY AND CONCLUSIONS

The theoretical analysis showed that unstiffened plates in bending which produces compression on their free edges sustain extremely severe reductions in their efficiency due to local buckling. The deflections become very large and the flexural rigidity reduces to a small fraction, less than 10% of its initial value. In view of this the strict limitations on the use of such elements beyond the local buckling load imposed in the current AISI Specification are well founded.

Stiffened bending elements, on the other hand, are not so severely effected by local buckling and have significant reserves of strength. The theoretical analysis indicated that the initial reduction in flexural rigidity at buckling was less than 30% at buckling, although this decreased further in the post-buckling range.

The method used in the papers to analyse sections was based on the theoretical results, was simple and routine in use, and avoided the complexities introduced by the effective width approach. Agreement with the experimental results of other authors was good.

TABLE 1

Case No.	K	$M_{CR}/\pi^2 D$	$E^*/_E (A^*/_A)$	$I^*/_I$	$\bar{y}^*/b$ (measured from the tension edge)
1	23.9	3.96	0.54	0.71	0.358
2	39.5	6.58	0.595	0.77	0.395
3	1.30	0.217	0.451	0.090	0.196
4	2.10	0.35	0.567	0.137	0.269

REFERENCES

1. Baehre, R 'Sheet Metal Panels for Use in Building' Proc. Third International Specialty Conference on Cold-Formed Steel Structures. St Louis 1975.

2. Bergfelt, A Edlund, B and Larsson, H. 'Experiments on The Trapezoidal Steel Sheets in Bending' Proc. Third International Specialty Conference on Cold-Formed Steel Structures. St Louis 1975.

3. Bergfelt, A Edlund, B 'Effects of Web Buckling in Light Gauge Steel Beams' Thin-Walled Structures, Edited by J Rhodes and A C Walker. Granada Publications 1980.

4. La Boube, R,A and Yu, W.W. 'Study of Cold-Formed Steel Beam Webs Subjected to Bending Stress' Proc. Third International Specialty Conference on Cold-Formed Steel Structures, St Louis 1975.

5. De Wolfe, J.T and Gladding C.J. ' Web Buckling in Beams' Proc. Fourth International Specialty Conference on Cold-Formed Steel Structures, St Louis 1976.

6. American Iron and Steel Institute 'Specification for the Design of Cold-Formed Steel Structural Members,' 1980.

7. Rhodes,J and Harvey, J.M. 'Plates in Uniaxial Compression With Various Support Conditions at the Unloaded Boundaries' Int. J. Mech. Sci. Vol 13, 1971.

8. Rhodes, J, Harvey, J.M. and Fok W.C 'The Load Carrying Capacity of Initially Imperfect Eccentrically Loaded Plates.' Int. J. Mech. Sci. Vol 17, 1975.

9. Rhodes J, Harvey, J.M. 'Interaction Behaviour of Plain Channel Columns Under Concentric or Eccentric Loading' Preliminary Report. 2nd Int. Colloqium on Stability of Steel Structures, Liege 1977

10. Rhodes, J and Harvey, J.M. 'The Local Buckling and Post Local Buckling Behaviour of Thin-Walled Beams' Aero Quarterly Nov 1971.

11. Rhodes, J and Harvey, J.M. 'Alternative Approach to Light Gage Beam Design.' Proc. ASCE. Journal of the Structural Division Vol 97 No ST8 1971.

NOTATION

A	=	Area of bending element
a	=	Buckle half wavelength
b	=	Element width
E	=	Young's modulus of Elasticity
I	=	2nd moment of Area
K	=	Buckling coefficient
M	=	Bending moment
P	=	Applied Load
t	=	Plate thickness
R	=	Radius of curvature
u^*	=	Compressional displacement of element compression edge
w	=	Magnitude of local deflections
$\bar{y}$	=	Distance from plate edge to neutral axis
α	=	Compression eccentricity factor
ν	=	Poisson's ratio - taken as 0.3
σ^*	=	Stress on element compression edge
$\bar{\sigma}_x$	=	Non dimensional value of stress $\left(= \sigma_x^* \times 12\frac{(1-\nu^2)\, b^2}{\pi^2\, Et^2}\right)$
σ_Y	=	Yield stress
M_{CR}, P_{CR}, u_{CR}, σ_{CR}	=	Critical values of M, P, u^* and σ^* respectively
M_{max}	=	Maximum moment on section
A^*, E^*, I^*, $\bar{y}^*$	=	Tangent values of A, E, I and $\bar{y}$ in the post-buckling range
A_{eff}, E_{eff}, I_{eff}, $\bar{y}_{eff}$	=	Effective values of A, E, I and $\bar{y}$

Figure Captions

Fig.1 Element dimensions and loading system

Fig.2 Variation of Buckling Coefficients with buckle length

Fig.3 Deflected forms across the element

Fig.4 Stress variations across the element

Fig.5 Variation of maximum deflection with applied moment

Fig.6 Moment-curvature variations

Fig.7 Effects of change of buckle length on moment-curvature variations

Fig.8 Comparison of theoretical and experimental failure moments for sections with equal area tension and compression flanges

Fig.9 Comparison of theoretical and experimental failure moments for sections of arbitrary tension/compression flange area ratios

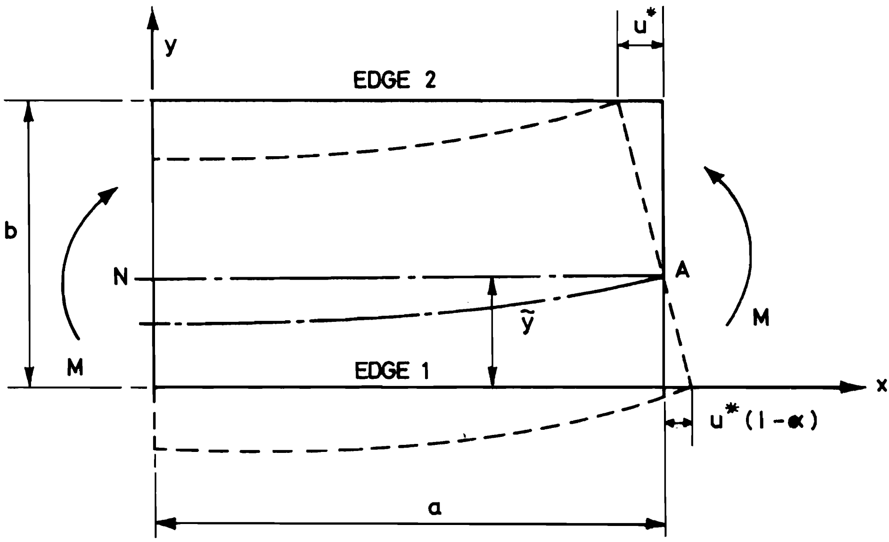

FIG. 1

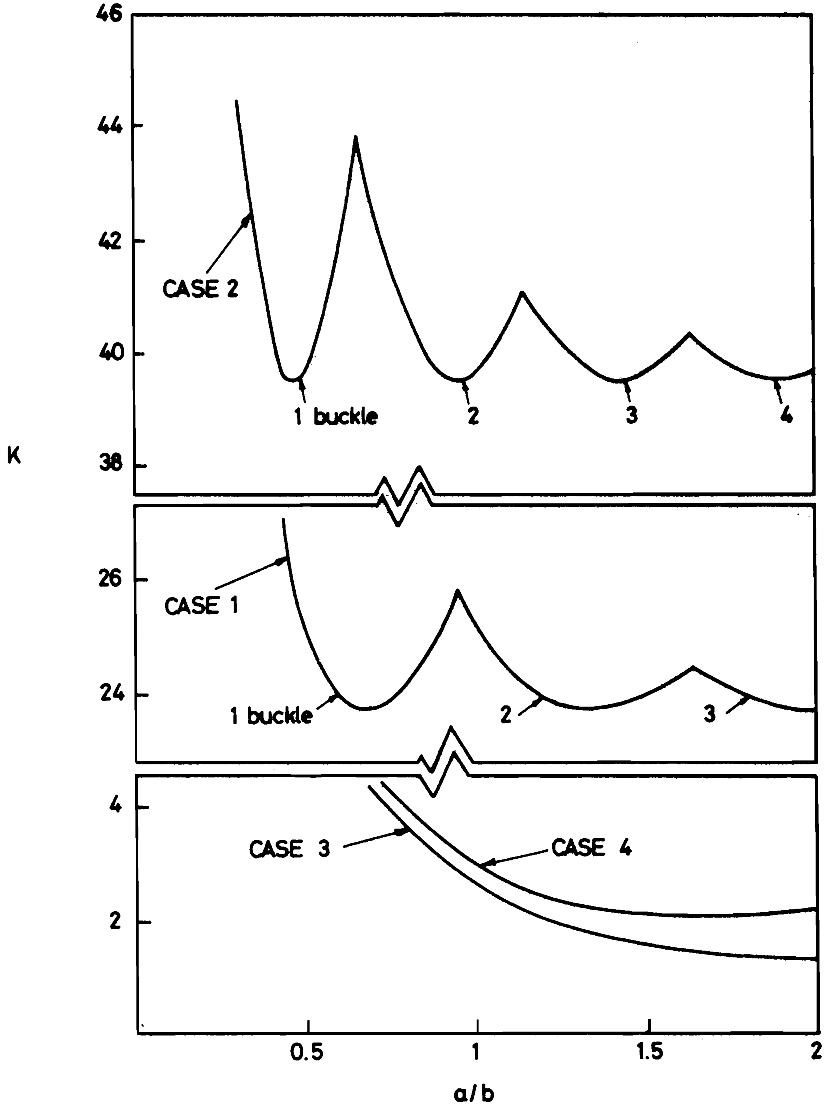
46
44
42
40
38
26
24
4
2
K
CASE 2
1 buckle
2
3
4
CASE 1
1 buckle
2
3
CASE 3
CASE 4
0.5
1
1.5
2
a/b

FIG. 2

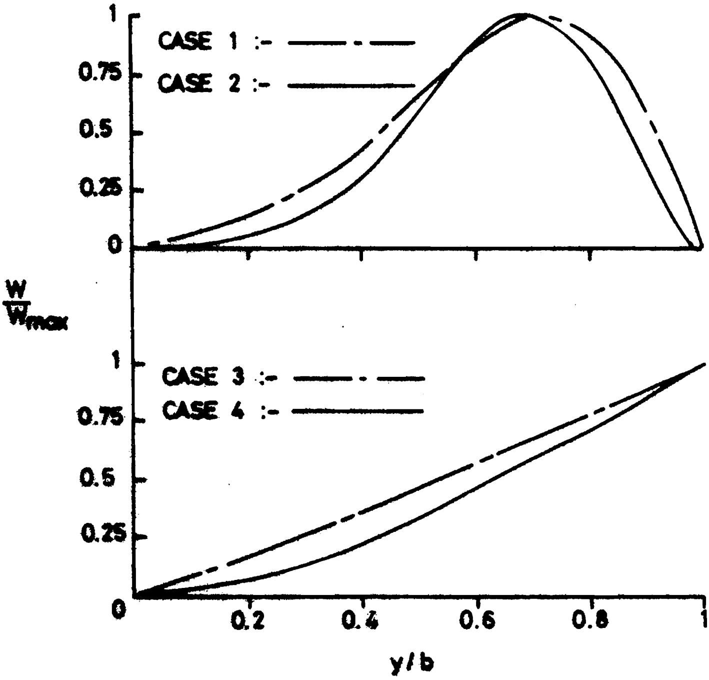

FIG. 3

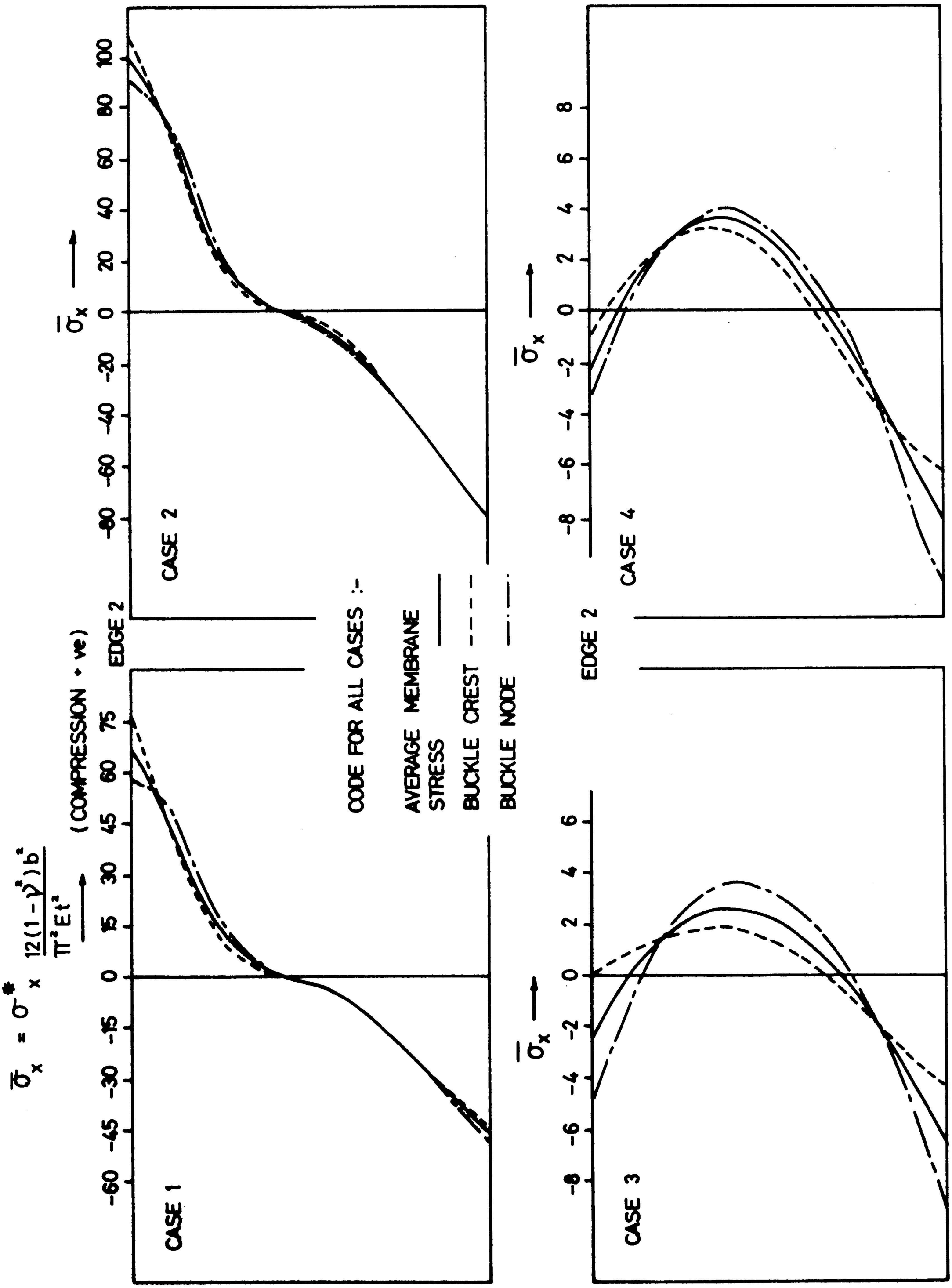
$\overline{\sigma}_x = \sigma^*_x \times \frac{12(1-\nu^2)b^2}{\pi^2 E t^2}$
(COMPRESSION + ve)
CODE FOR ALL CASES :-
AVERAGE MEMBRANE STRESS
BUCKLE CREST
BUCKLE NODE
EDGE 2
CASE 1
CASE 2
CASE 3
CASE 4
$\overline{\sigma}_x$

FIG. 4

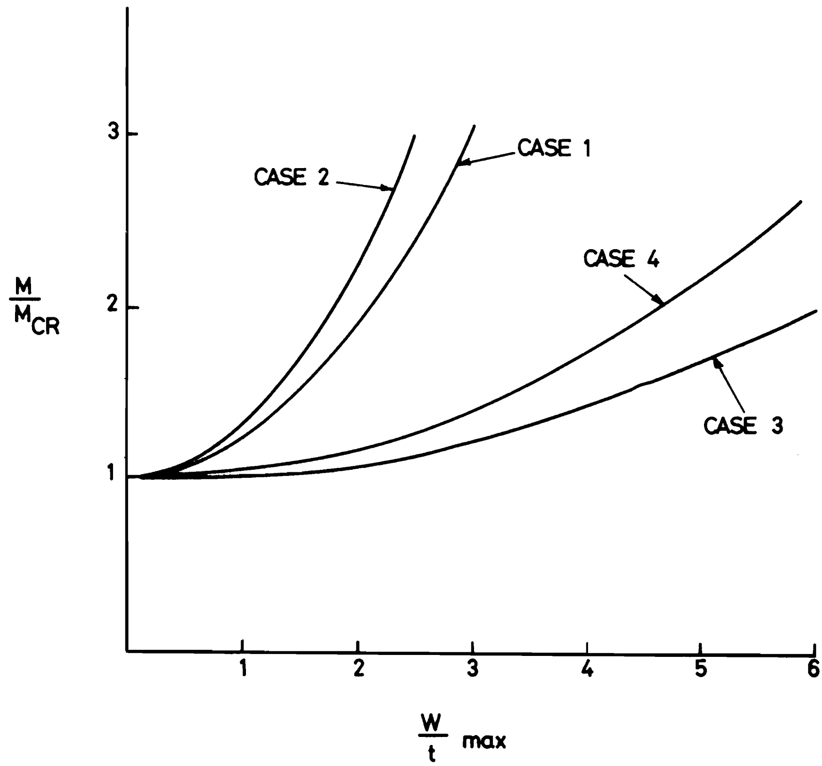

FIG. 5

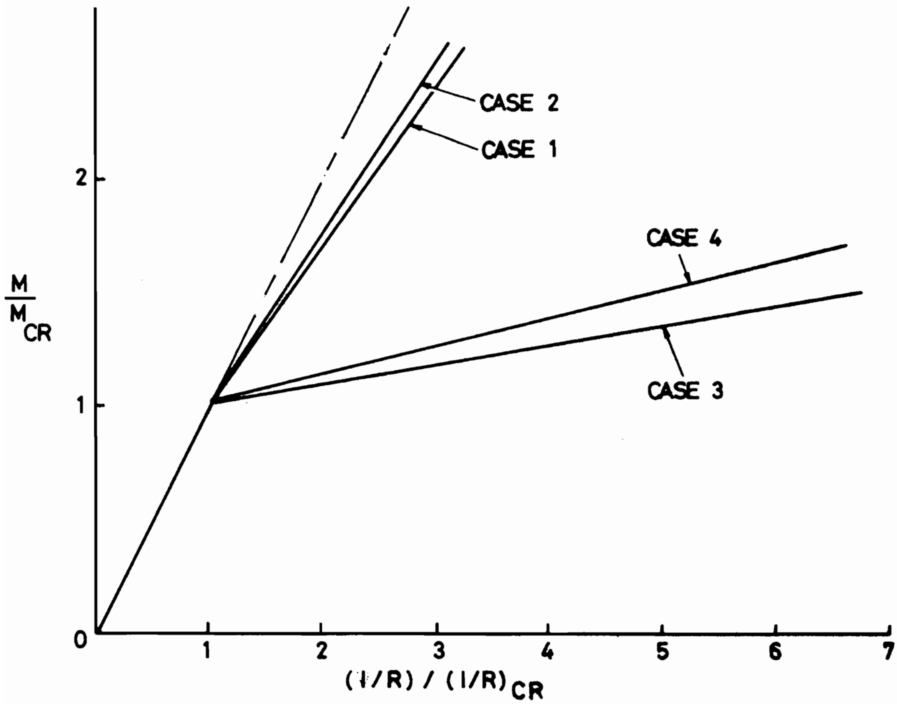
CASE 2
CASE 1
CASE 4
CASE 3
2
1
0
1 2 3 4 5 6 7
$\frac{M}{M_{CR}}$
$(1/R) / (1/R)_{CR}$

FIG. 6

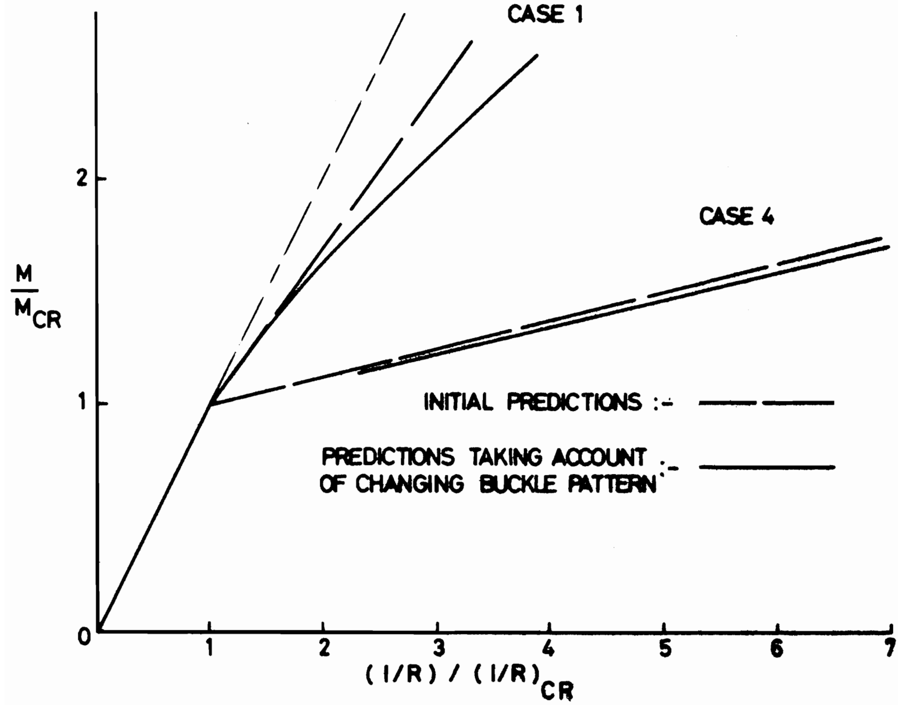
CASE 1
CASE 4
INITIAL PREDICTIONS :-
PREDICTIONS TAKING ACCOUNT OF CHANGING BUCKLE PATTERN :-
2
1
0
1 2 3 4 5 6 7
$\frac{M}{M_{CR}}$
$(1/R) / (1/R)_{CR}$

FIG. 7

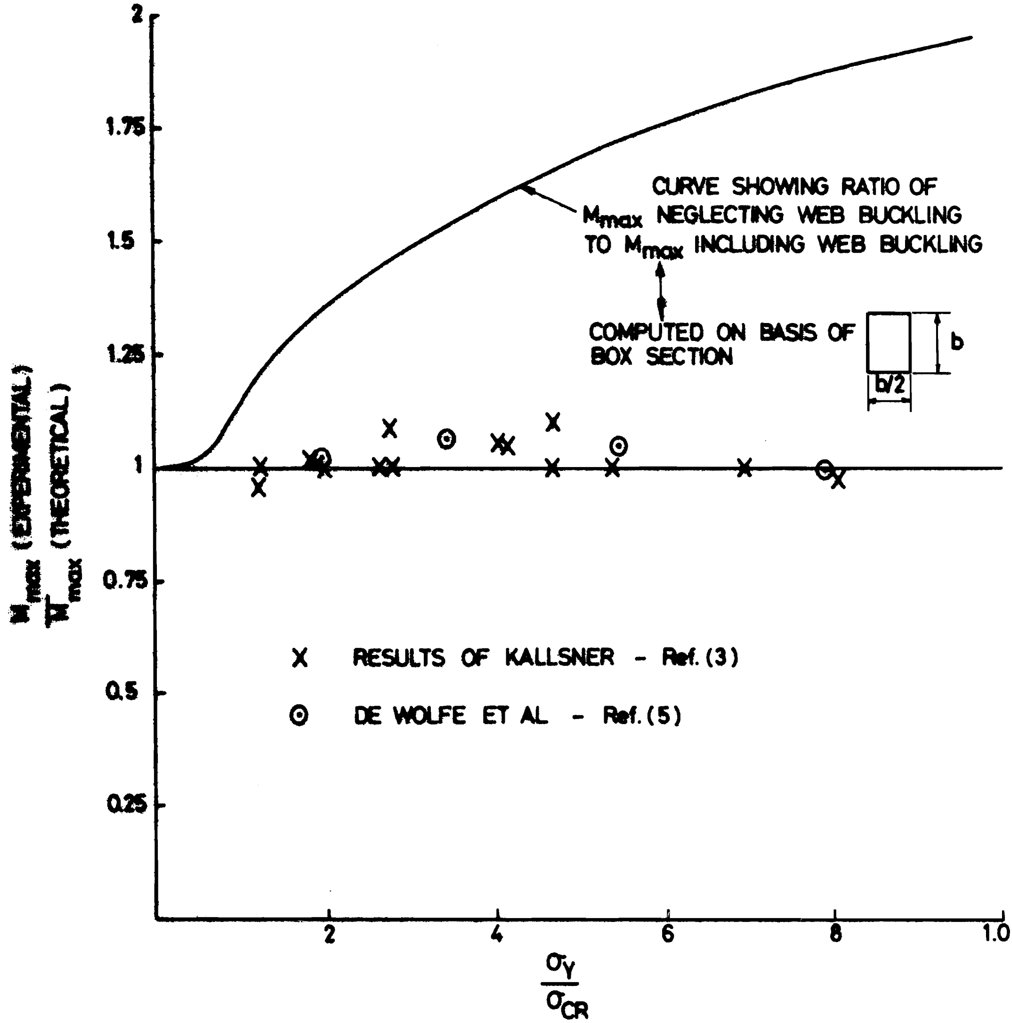

2
1.75
1.5
1.25
1
0.75
0.5
0.25
M max (EXPERIMENTAL)
M max (THEORETICAL)
CURVE SHOWING RATIO OF
M max NEGLECTING WEB BUCKLING
TO M max INCLUDING WEB BUCKLING
COMPUTED ON BASIS OF
BOX SECTION
b
b/2
X RESULTS OF KALLSNER - Ref. (3)
DE WOLFE ET AL - Ref. (5)
2
4
6
8
1.0
σY / σCR

FIG. 8

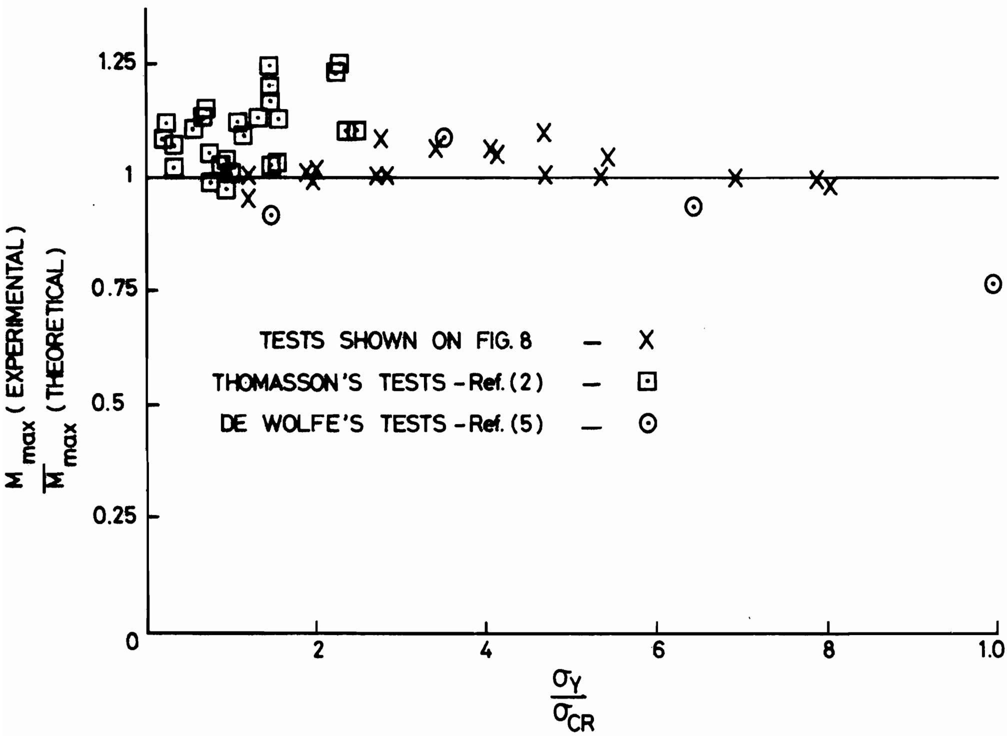
1.25
1
0.75
0.5
0.25
0
2
4
6
8
1.0
M_{max} (EXPERIMENTAL)
$\overline{M}_{max}$ (THEORETICAL)
$\frac{\sigma_Y}{\sigma_{CR}}$
TESTS SHOWN ON FIG. 8 — X
THOMASSON'S TESTS - Ref. (2) — ⊡
DE WOLFE'S TESTS - Ref. (5) — ⊙

FIG. 9